AFRL-RZ-WP-TP-2010-2250

OPTICAL MEASUREMENTS OF PRESSURE AND SHEAR ON A STRUT IN SUPERSONIC FLOW (POSTPRINT)

Jim Crafton, Sergey Fonov, and Kuang-Yu Hsu

Innovative Scientific Solutions, Inc.

Campbell D. Carter and Mark R. Gruber

Propulsion Sciences Branch
Aerospace Propulsion Division

AUGUST 2009

AIR FORCE RESEARCH LABORATORY
PROPULSION DIRECTORATE
WRIGHT-PATTERSON AIR FORCE BASE, OH 45433-7251
AIR FORCE MATERIEL COMMAND
UNITED STATES AIR FORCE

REPORT DOCUMENTATION PAGE

Form Approved
OMB No. 0704-0188

1. REPORT DATE *(DD-MM-YY)*
August 2009

2. REPORT TYPE
Conference Paper Postprint

3. DATES COVERED *(From - To)*
01 August 2008 – 31 August 2009

4. TITLE AND SUBTITLE
OPTICAL MEASUREMENTS OF PRESSURE AND SHEAR ON A STRUT IN SUPERSONIC FLOW (POSTPRINT)

5a. CONTRACT NUMBER
In-house

5b. GRANT NUMBER

5c. PROGRAM ELEMENT NUMBER
62203F

6. AUTHOR(S)
Jim Crafton, Sergey Fonov, and Kuang-Yu Hsu (Innovative Scientific Solutions, Inc.)
Campbell D. Carter and Mark R. Gruber (AFRL/RZAS)

5d. PROJECT NUMBER
3012

5e. TASK NUMBER
AI

5f. WORK UNIT NUMBER
3012AI00

7. PERFORMING ORGANIZATION NAME(S) AND ADDRESS(ES)

Innovative Scientific Solutions, Inc.
Dayton, OH 45440

Propulsion Sciences Branch (AFRL/RZAS)
Aerospace Propulsion Division
Air Force Research Laboratory, Propulsion Directorate
Wright-Patterson Air Force Base, OH 45433-7251
Air Force Materiel Command, United States Air Force

8. PERFORMING ORGANIZATION REPORT NUMBER
AFRL-RZ-WP-TP-2010-2250

9. SPONSORING/MONITORING AGENCY NAME(S) AND ADDRESS(ES)
Air Force Research Laboratory
Propulsion Directorate
Wright-Patterson Air Force Base, OH 45433-7251
Air Force Materiel Command
United States Air Force

10. SPONSORING/MONITORING AGENCY ACRONYM(S)
AFRL/RZAS

11. SPONSORING/MONITORING AGENCY REPORT NUMBER(S)
AFRL-RZ-WP-TP-2010-2250

12. DISTRIBUTION/AVAILABILITY STATEMENT
Approved for public release; distribution unlimited.

13. SUPPLEMENTARY NOTES
Conference paper published in the *Proceedings of the 45th AIAA/ASME/SAE/ASEE Joint Propulsion Conference and Exhibit*, conference held August 2 - 5, 2009 in Denver, CO. This paper contains color. PA Case Number: 88ABW-2009-3029; Clearance Date: 01 Jul 2009.

The U.S. Government is joint author of this work and has the right to use, modify, reproduce, release, perform, display, or disclose the work.

14. ABSTRACT
To quickly vet candidate strut geometries, as well as build a database for computational validation, a series of struts was constructed and investigated with optical sensors for pressure, velocity, and skin friction. This paper reports the results of pressure and skin friction measurements on the strut surface using Pressure-Sensitive Paint (PSP) and Surface Stress Sensitive Films (S3F). PSP is an optical sensor that provides continuous distributions of pressure on a model surface. The paint on the surface is doped with a luminescent dye that is sensitive to the partial pressure of oxygen, and thus luminescent intensity is a function of pressure. S3F is a new skin friction sensor based on an elastic polymer film that deforms under the action of applied normal and tangential loads. Skin friction is determined by monitoring these deformations, and then solving an inverse problem using a finite element model of the elastic film.

15. SUBJECT TERMS
supersonic combustion, pressure-sensitive paint, shear-sensitive films

16. SECURITY CLASSIFICATION OF: a. REPORT	b. ABSTRACT	c. THIS PAGE	17. LIMITATION OF ABSTRACT:	18. NUMBER OF PAGES	19a. NAME OF RESPONSIBLE PERSON (Monitor)
Unclassified	Unclassified	Unclassified	SAR	16	Mark R. Gruber
					19b. TELEPHONE NUMBER *(Include Area Code)* N/A

Standard Form 298 (Rev. 8-98)
Prescribed by ANSI Std. Z39-18

45th AIAA/ASME/SAE/ASEE Joint Propulsion Conference & Exhibit
2 - 5 August 2009, Denver, Colorado

AIAA 2009-5033

Optical Measurements of Pressure and Shear on a Strut in Supersonic Flow

Jim Crafton[*], Sergey Fonov[†], and Kuang-Yu Hsu[†]
Innovative Scientific Solutions, Inc., Dayton, Ohio, 45440

and

Campbell D. Carter[‡] and Mark R. Gruber[‡]
Air Force Research Laboratory (AFRL/RZAS), Propulsion Directorate, OH 45433

To quickly vet candidate strut geometries, as well as build a database for computational validation, a series of struts was constructed and investigated with optical sensors for pressure, velocity, and skin friction. This paper reports the results of pressure and skin friction measurements on the strut surface using Pressure-Sensitive Paint (PSP) and Surface Stress Sensitive Films (S3F). PSP is an optical sensor that provides continuous distributions of pressure on a model surface. The paint on the surface is doped with a luminescent dye that is sensitive to the partial pressure of oxygen, and thus luminescent intensity is a function of pressure. S3F is a new skin friction sensor based on an elastic polymer film that deforms under the action of applied normal and tangential loads. Skin friction is determined by monitoring these deformations, and then solving an inverse problem using a finite element model of the elastic film.

I. Introduction

EXPERIMENTAL measurements are commonly used to analyze a flow field, or as a basis for validating computational models. Surface data such as pressure, skin friction, and heat transfer can be particularly useful for these purposes. Traditional techniques for acquiring measurements of surface temperature and pressure on wind tunnel models have utilized embedded arrays of thermocouples and pressure taps. This approach requires significant model construction and setup time while producing data with limited spatial resolution. Furthermore, physical constraints such as mechanical movement or section thickness can preclude the use of thermocouples and pressure taps in certain regions of a model, for example near a thin leading or trailing edge. An alternative approach is the use of luminescent probes that are sensitive to temperature and pressure. This technique, known as Temperature and Pressure-Sensitive Paint[1], (TSP/PSP) has produced high spatial resolution measurements of temperature and pressure on surfaces that have in the past proven to be inaccessible. Another sensor that is currently under development is Surface Stress Sensitive Films (S3F). This image-based sensor provides continuous distributions of skin friction on a surface. Experimental measurements of pressure and skin friction were obtained on several strut models in a supersonic test section using PSP and S3F. Strut injectors were evaluated as alternatives to fuel large-scale scramjets that can potentially improve the mixing and reduce overall engine length. A fundamental mixing study using various strut configurations in supersonic flow illustrated the influence of strut geometry on mixing performance[2]. The drag, structure, and heat transfer associated with struts in supersonic flows are also critical issues to be addressed for practical applications. The objective of this study is to investigate the surface pressure and shear distribution of strut in supersonic environment.

II. Experimental Descriptions

The overall objective of this study is to acquire experimental measurements of pressure, velocity, and skin friction on the surfaces of various strut configurations in supersonic flow. The results will provide a better understanding of aerodynamics of strut injectors, as well as for validation of computational models.

[*] Research Scientist, 2766 Indian Ripple Road, Dayton, OH 45440. AIAA Senior Member.
[†] Research Scientist, 2766 Indian Ripple Road, Dayton, OH 45440. AIAA Associate Fellow.
[‡] Principal. Aerospace Engineer, AFRL/RZAS, 1950 Fifth Street, WPAFB, OH 45433. AIAA Associate Fellow.

A. Research Facility

The experimental study was conducted in a direct-connect supersonic flow facility located at the U.S. Air Force Research Laboratory (Propulsion Directorate), Wright-Patterson AFB. Symmetric facility nozzles were used to produce supersonic flow at nominal Mach numbers of 2 and 3. Figure 1illustrates the test section and experimental setup. Windows are located on both side walls and the top wall for optical access. A pair of illumination sources and CCD cameras were aligned to obtain the side view and top view for both PSP and S3F measurements. Each system was composed of a PCO.1600 CCD camera with a Micro-Nikkor 55-mm Nikon lens, a 610-nm long-pass filter, and a PC running OMS Acquire™. Various struts were installed on the bottom wall of a constant-area (13.1 x 15.24 cm^2) test section. Examples of three strut models coated with PSP are shown in Figure 1

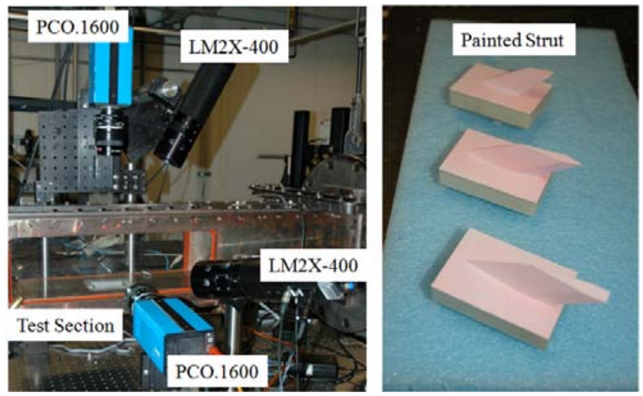

Figure 1. Experimental Setup and PSP-Coated Struts.

B. Pressure Sensitive Paint

Pressure-sensitive paint (PSP) is an image-based measurement technique that can produce continuous distributions of pressure on a surface. The fundamental operating principle of PSP is oxygen quenching of luminescence from the paint. The intensity of the light emitted by the paint is monitored using a camera, and this signal is inversely proportional to the local barometric pressure. The primary advantages of PSP over traditional, point-measurement techniques are high spatial resolution and the ability to instrument difficult locations such as thin trailing edges and control surfaces. A comprehensive review of Pressure-Sensitive Paint is given by Liu and Sullivan[1], while a basic overview of the technique is given here.

Image based pressure measurements using PSP are accomplished by coating the model surface with the paint and illuminating the surface with light of the appropriate wavelength that will excite the paint luminescence. The surface is imaged through a long-pass filter to separate the luminescence from the excitation light. A schematic of the system is shown in Figure 2. Unfortunately, the luminescence from the paint is not only a function of pressure. The luminescence also varies with illumination intensity, probe concentration, paint layer thickness, and detector sensitivity. These spatial variations result in a non-uniform luminescence from the painted surface. The spatial variations are eliminated by taking the ratio of the luminescent intensity of the paint at an unknown test condition, I, with the luminescent intensity of the paint at a known reference condition, I_o. This wind-off/wind-on ratio is then a function of the local barometric pressure.

Sources of uncertainty for PSP measurements have been investigated and modeled by Liu and Sullivan[1]. These error sources include temperature, illumination, model displacement and deformation, sedimentation, photo-degradation, and camera shot noise. Liu concluded that the major sources of error for most PSP tests were temperature and illumination. The relationship between surface illumination and paint luminescence is linear; therefore, any change in surface illumination will result in an equal change in paint luminescence. Generally, this change is surface illumination is the result of model movement between the wind-off and wind-on images. As the model changes position, the distance between any point on the airfoil surface and the fixed PSP lighting will vary. The relationship between illumination intensity at a point on the surface and the distance between the PSP lighting and the point of interest are an inverse function of the distance squared. The result is an error in the PSP measurement that is a function of the model movement. This error, however, can be eliminated by using a Binary PSP.

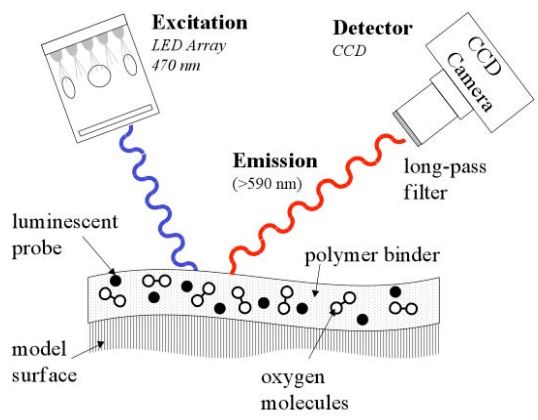

Figure 2. Basic PSP System.

A Binary PSP deals with the issue of illumination errors by employing a reference probe. In fact, several groups have successfully demonstrated this approach[3 4]. The goal is to use the luminescence of the reference probe to correct for variations in the luminescence of the signal probe (the pressure sensor) that is caused by variations in illumination. This is accomplished by taking a ratio of the luminescence of the signal probe to the luminescence of the reference probe. Since the luminescent signal from each probe is a linear function of the illuminations, the ratio of the signals from the probes naturally eliminates illumination variations from the equation. In the case of Binary FIB[5], the reference probe is also used to minimize the temperature sensitivity of the system, a second major source of error identified by Liu. A calibration of Binary FIB, demonstrating this low sensitivity to temperature, is given in Figure 3.

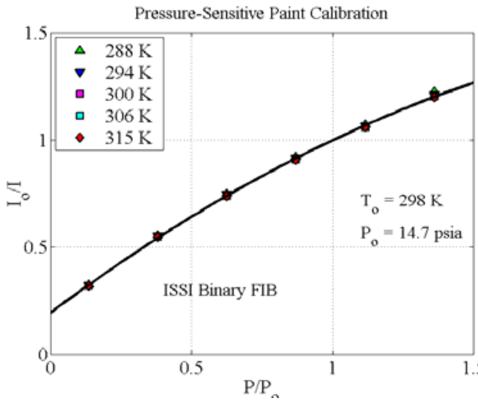

Figure 3. Binary FIB Calibration.

Generally, it is useful to compare the processed PSP pressure data to several pressure taps on the model. This in-situ correction procedure can be carried out on the bitmaps; however, this requires that the pressure taps be clearly visible on the bitmap. A more general approach involves mapping the PSP images onto a three-dimensional surface mesh of the model. This resection procedure can be accomplished either automatically, using well defined surface markers, or interactively, using tools in the ProField software suite. Once the data is mapped onto the surface mesh, it can be compared to pressure taps on the model, computational results, or combined with other experimental data for analysis. The PSP data presented in this report has undergone the resection procedure and the results are presented on the mesh of each model.

C. Surface Stress Sensitive Film

Measurement of surface shear stress or skin friction is a challenge in aerodynamic applications. Current techniques to measure skin friction can require the use of mechanical balances, intrusive probes and sensors, or a variety of surface mounted substances. A review of the literature yields a variety of techniques including oil films[6], liquid crystals[7, 8], thermal sensors[6], an array of MEMS based sensors[9], and near-wall velocity sensors[10, 11]. Recently a new technique for measurement of skin friction has been introduced. The basis of this measurement is an elastic film that deforms under the action of applied loads. The reaction of the film to the loads is monitored using imaging and modeled using finite element analysis resulting in a continuous distribution of skin friction over the film surface. This technique is known as Surface Stress Sensitive Films[12] (S3F).

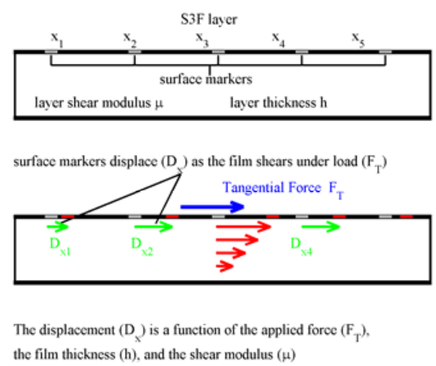

Figure 4. Response of S3F to a Tangential Load.

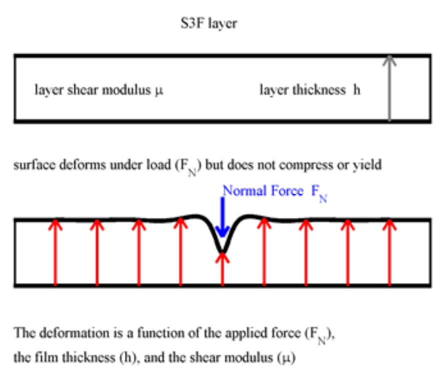

Figure 5. Response of S3F to a Normal Load.

Some insight into the operation of the S3F is gained by considering the simplified response of the film to normal and tangential forces. The response of the film to a tangential force, F_T, is depicted in Figure 4. Here, the surface of the film will undergo a tangential displacement (D_X) due to the load (F_T) but will not yield or compress. The response of the film may be visualized by considering a series of markers on the surface of the film. The markers will be displaced as the film shears and this displacement is a function of the film thickness (h) and shear modulus (μ). Upon removal of the load, the film will return to its original shape.

The response to a normal force is depicted in Figure 5. The film will deform under the normal load but will not compress or yield. The local thickness of the film will be modified by the presence of the load near the point of action. Upon removal of the load, the film will return to its original shape. The maximum surface displacement is a function of the material properties and the applied normal load. Materials are typically formulated to produce deflection of less than 5% of total material thickness under the anticipated maximum loading, and can be produced to provide less than 1% deflection. The stressed film thickness is a function of the applied normal force (F_N), the original thickness of the film (h), and its shear modulus (μ).

The actual response of the film is more complex as the responses are mildly coupled: a pure tangential load will generate a slight change in film thickness and a pure normal load will generate a slight tangential displacement. These simplified examples however demonstrate the basic operation of the S3F. One final property of interest is the film's frequency response and potential as a high-frequency probe for both skin friction and pressure. The range of the linear frequency response of an elastic layer is limited by the natural frequency, f_o, of the tangential oscillation. This can be estimated as

$$f_0 = \frac{1}{2\pi}\sqrt{\frac{\mu}{\rho\, \mathrm{h}^2}} \tag{1}$$

where ρ is the film density. By adjusting the shear modulus (μ from 100-Pa to 5000-Pa) and thickness (h from 0.1-mm to 1-mm) it is possible to adjust the frequency response of the film from 50-Hz to 3.5-kHz. To date, films with frequency response of over 1-kHz have been demonstrated.

In order for a S3F sensor to produce the desired results it must be applied to the surface under study. There are several ways for films to be applied to a surface including spraying with an airbrush, allowing the film to polymerize in a cavity on the model surface, or forming the film in a cavity on a flexible layer which can be glued onto a model surface. Forming films in cavities provides good control of the film thickness and shear modulus, and of course control of these parameters is necessary for quantitative measurement of pressure and skin friction. Film formation consists of pouring the polymer components into a flat cavity with a smooth or polished bottom and allowing the film to polymerize. The film thickness can be estimated by direct measurements using either optical absorption or an ultrasonic or capacitive thickness gauge.

The film calibration procedure involves applying a specified load to the film surface and measuring the corresponding normal and tangential deformation of the film. An example of the calibration setup is shown in Figure 6. A small weight is placed on the film and the displacement of the weight is monitored as the calibration system is rotated. The tangential force (shear force) of the weight is a function of the weight and angle at which the plate is tilted. The displacement of the weight is plotted versus the applied force and the shear modulus is computed as the slope of this curve using the equation in Figure 6.

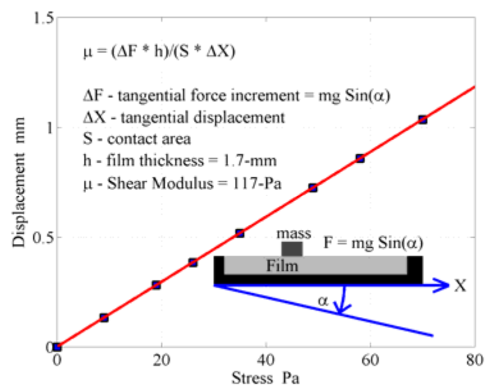

Figure 6. Calibration using Static Shear Loading.

To evaluate the quantitative accuracy of the S3F, an experiment was performed using a fully developed channel. The fully developed channel flow provides an excellent environment for validating the S3F sensor for skin friction measurements. The skin friction in the channel may be determined experimentally by monitoring the pressure gradient[13] (Equation 2) or theoretically by monitoring the Reynolds Number and using the Poiseuille[13] flow relation (Equation 2).

$$\tau_w = -\frac{H}{2}\left(\frac{dP}{dx}\right) \qquad\qquad C_f = \frac{24}{\mathrm{Re}_{DH}} \tag{2}$$

These theoretical and experimental results can be compared to the results obtained from the S3F, and some measure of validation of the skin friction measurements can be obtained.

The channel is created using a cavity of 150-mm length by 24-mm width by 1.72-mm depth. The acrylic cover plate includes two ports for air inlet/outlet as well as two ports for monitoring the pressure gradient, placed about 150 channel heights (h) downstream of the inflow port. The film is imaged in the region between the pressure ports using a PCO.1600 CCD camera. Data was acquired at several flow rates while the pressure gradient was monitored

using a Validyne (CD379) pressure transducer. The flow rate was set using a mass flow controller (Alicat, MC series) and thus the Reynolds Number could be determined. Data was acquired using two relatively thick films (~300-μm) with shear modulus 312-Pa and 3035-Pa.

The S3F and pressure gradient skin friction measurements are plotted versus Reynolds number in Figure 7, along with the Poiseuille flow relation. The skin frictions in Figure 7 range from 1-Pa to 50-Pa. The pressure gradient, Poiseuille flow, and S3F skin friction measurements are in good agreement (better than 3% full scale) over the range of skin frictions encountered in this flow. These results demonstrate that the S3F can be used for quantitative skin friction measurements.

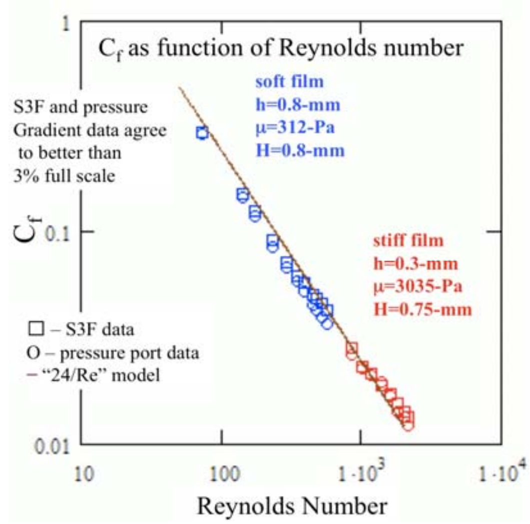

Figure 7. Skin Friction Coefficient as a Function of Reynolds Number for a Fully-Developed Channel.

III. Results

The results of surface pressure and skin friction on selected struts are reported here. Surface pressure distributions on Strut A in a Mach 2 flow is illustrated in Figure 8. A high pressure zone at the thin leading edge of the strut due to the flow impingement is clearly identified in Figure 8a. The low pressure region behind the expansion is also observed in the image. The flow expansion (indicated by the low pressure) is larger toward the tip of the strut and is smaller near the floor as would be expected due to the pressure relief over the top of the strut.

As these struts are under investigation for supersonic fueling methods, there are several fuel injection ports evident on the surface. An interesting use of PSP is as a flow visualization tool. Here Nitrogen (N_2) was injected through the injection ports; the resulting pressure field (Figure 8b) is indicitive of both pressure and mass fraction of injected gas. A pair of bow shocks are formed in front of the injection ports as would be expected. The trace of the injected N_2 near the strut surface is identified by the low pressure region behind the injection ports. These regions are not actually at low pressure but the result of the the replacement of O_2 by the injected N_2. The presence of the gas on the surface would indicate that some of the injected gas should enter the stagnant subsonic zone behind the strut, and therefore, possibly be available for combustion and flame holding. Similar data was collected on other struts, this data is presented in Appendix A.

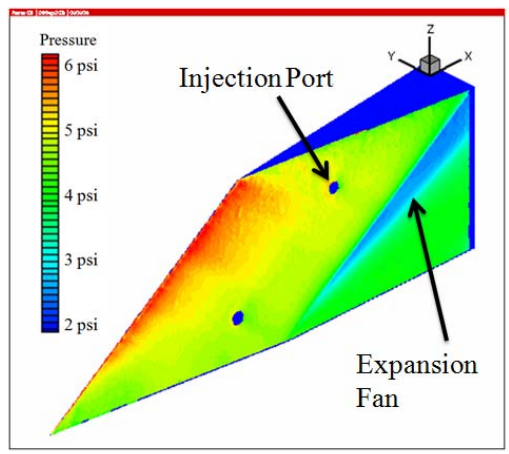

(a) No N_2 injection

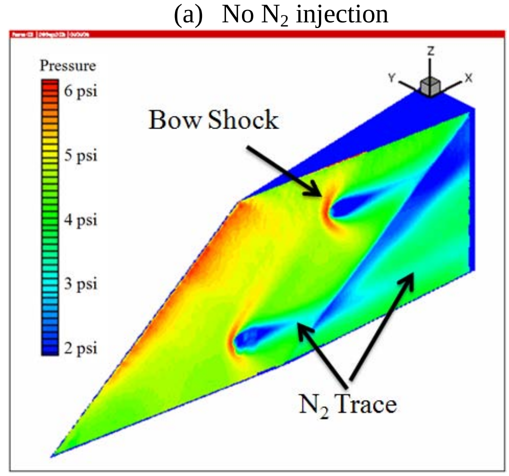

(b) N_2 injection

Figure 8. Pressure Distributions on Strut A.

The surface skin friction and pressure distribution on Strut B at Mach 2 is shown in Figure 9. Strut B is a truncated version of Strut A, basically a simple triangular-shape strut. The pressure distribution (Figure 9a) is similar to the leading edge of Strut A, with high pressure near the leading edge and lower pressure along the chord. Surface streamlines, reduced from the skin friction data, superimposed on a color map that indicates the magnitude of shear is illustrated in Figure 9b. Note the similarity between the pressure field and the skin friction. The skin friction is directed along the pressure gradient perpendicular to the leading edge, then the surface flow turns and moves parallel. It is interesting to note that the surface flow has both positive and negative components in the transverse direction.

Among the uses of the experimental data produced by PSP and S3F are analysis of the flow and validation of computational models. To facilitate this type of analysis, the data can be mapped onto the surface mesh and combined. In this case, the combined data is comprised of pressure distributions and skin friction vectors. Data of this type is presented here for Strut A in Figure 10. Here we have focused on the region around one of the injectors while N_2 is being injected into the flow. The color map indicates the pressure from PSP and the vectors represent the skin friction from the S3F. This combined view of the data indicates the location of the bow shock (PSP) and the relative location of the saddle point upstream of the bow shock (S3F). The vectors show the surface flow turning abruptly and wrapping around the bow shock while behind the shock, the flow is actually reversed. About one jet diameter behind the injector, the shear drops dramatically and the flow seems to stagnate on the surface, even though no abrupt change is evident in the pressure distribution.

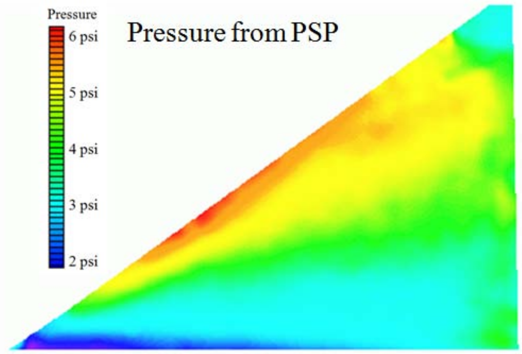

(a) Pressure

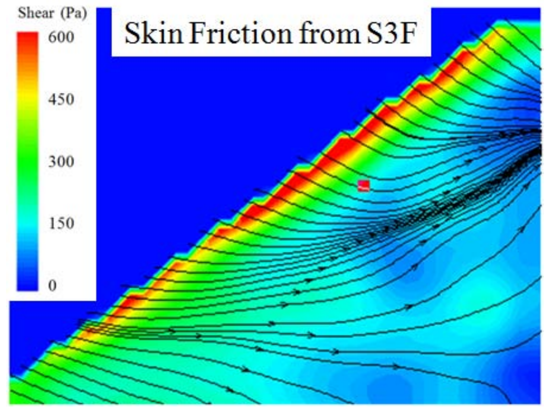

(b) Skin Friction

Figure 9. Shear and Pressure on Strut B.

IV. Summary

Surface pressure and skin friction distributions on various strut injectors in supersonic flows are measured using PSP and S3F techniques. Details of these quantitative surface measurement techniques are described. Results showed high-pressure region in the leading edge and flow expansion on the side of struts. PSP and N_2 injection illustrate the bow shocks ahead of injection ports and traces of injectant along the strut surface. Surface streamlines reduced from the skin friction data reveals the interesting flow features that provide important insight for strut injector design. Collected PSP and skin friction data can be mapped onto the surface mesh and the combined data of pressure distributions and skin friction vectors can be used for CFD validation.

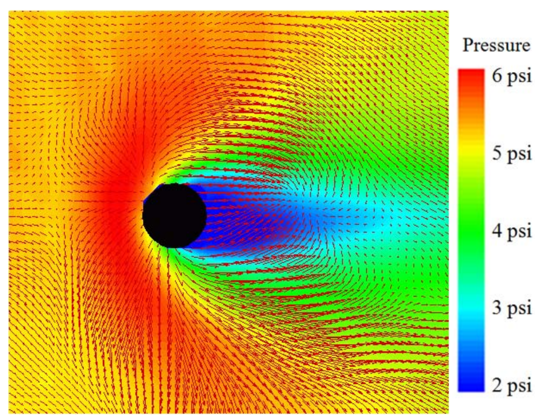

Figure 10. Combined PSP and S3F Data.

Acknowledgments

This work was sponsored by the AFRL Propulsion Directorate under Contract FA8650-08-D-2845. The authors would like to thank Mr. Robert Behdadnia for his support. The assistance of Messrs. G. Streby, D. Schommer, and W. Terry in preparing and conducting experiments is also appreciated. The support of the Research Air Facility of AFRL/RZ is also acknowledged.

References

1 Liu T and Sullivan JP, "Pressure and Temperature Sensitive Paints", Springer-Verlag, (2004)
2 Hsu K-Y, Carter C, Gruber M, and Tam, C. –J., “Mixing Study of Strut Injectors on Supersonic Flows,” to be presented at 45th AIAA/ASME/SAE/ASEE Joint Propulsion Conference & Exhibit, Denver ,Co, 2-5 August (2009)
3 Bykov A, Fonov S, Mosharov V, Orlov A, Pesetsky V, Radchenko V. Study Result for the Application of Two-component PSP Technology to Aerodynamic Experiment. AGARD'97
4 Khalil G, Costin C, Crafton J, Jones E, Grenoble S, Gouterman M, Callis J, Dalton L “Dual Luminophor Pressure Sensitive Paint I: Ratio of Reference to Sensor Giving a Small Temperature Dependence” Sensors and Actuators B, Vol. 97, n 1, pp. 13-21
5 Crafton J, Fonov S, Jones E, Fonov V, Goss L, “Simultaneous Measurements of Pressure and Deformation on a UCAV in the SARL”, AIAA-2005-1028

6 Goldstein, Fluid Mechanics Measurements, Taylor & Francis, 1996.
7 Reda DC, Wilder MC, Mehta RD, and Zilliac G "Measurements of continuous pressure and shear distributions using coating and imaging techniques," AIAA Journal, 36:895-9, 1998.
8 Zhong S, "Detection of flow separation and reattachment using shear-sensitive liquid crystals," Experiment in Fluids, 32:667-73, 2002.
9 Sheplak M, Cattafesta L, and Nishida T, "MEMS Shear Stress Sensors: Promise and Progress," AIAA-2004-2026.
10 Hochareon P, Manning KB, Fontaine A, Tarbell JM, and Deutsch S, "Wall shear-rate estimation within the 50cc Penn State Artificial Heart using particle image velocimetry," ASME J Biomech. Eng., 126:430-37, 2004.
11 Fourguette, D., Modarress, D., Wilson, D., Koochesfahani, M., and Gharib, M., "An Optical MEMS-Based Shear Stress Sensor for High Reynolds Number Applications," AIAA-03-0742, Reno, January 2003.
12 Fonov S, Jones E, Crafton J, Fonov V, Goss L, "The development of optical techniques for the measurement of pressure and skin friction", Measurement Science and Technology, Vol. 17, pp. 1261-1268 (2006)
13 Schlichting, Gersten, Krause, Oertel, Mayes "Boundary-Layer Theory" 8th edition Springer (2004)

Appendix A: Summary of Pressure Paint Data

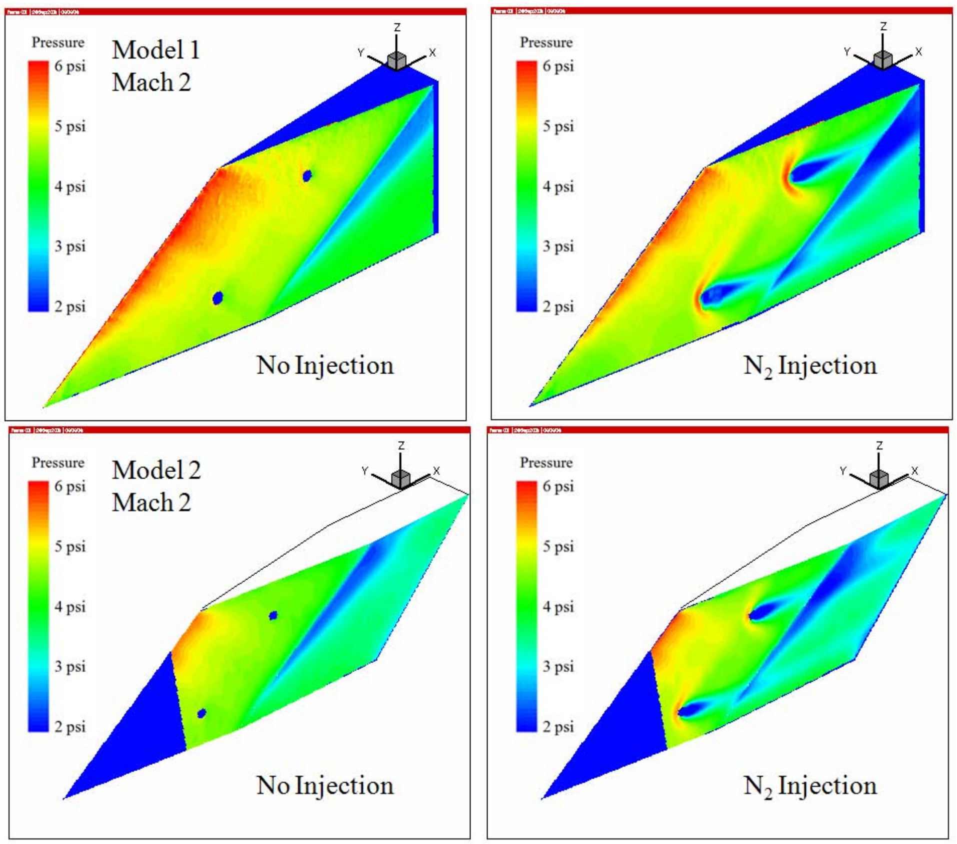

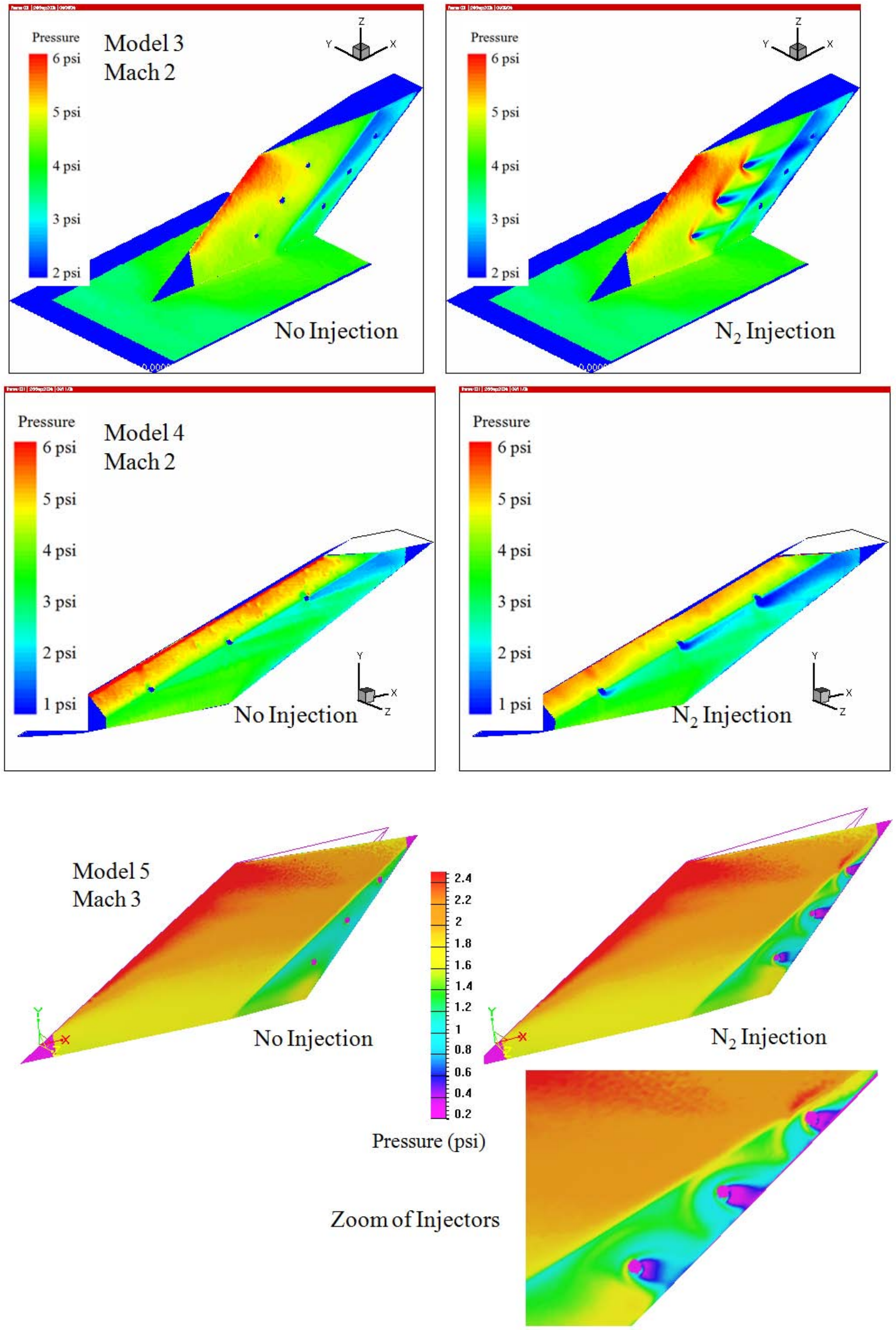
Pressure
6 psi
5 psi
4 psi
3 psi
2 psi
Model 3
Mach 2
No Injection
N2 Injection
Pressure
6 psi
5 psi
4 psi
3 psi
2 psi
1 psi
Model 4
Mach 2
No Injection
N2 Injection
Model 5
Mach 3
No Injection
N2 Injection
2.4
2.2
2
1.8
1.6
1.4
1.2
1
0.8
0.6
0.4
0.2
Pressure (psi)
Zoom of Injectors

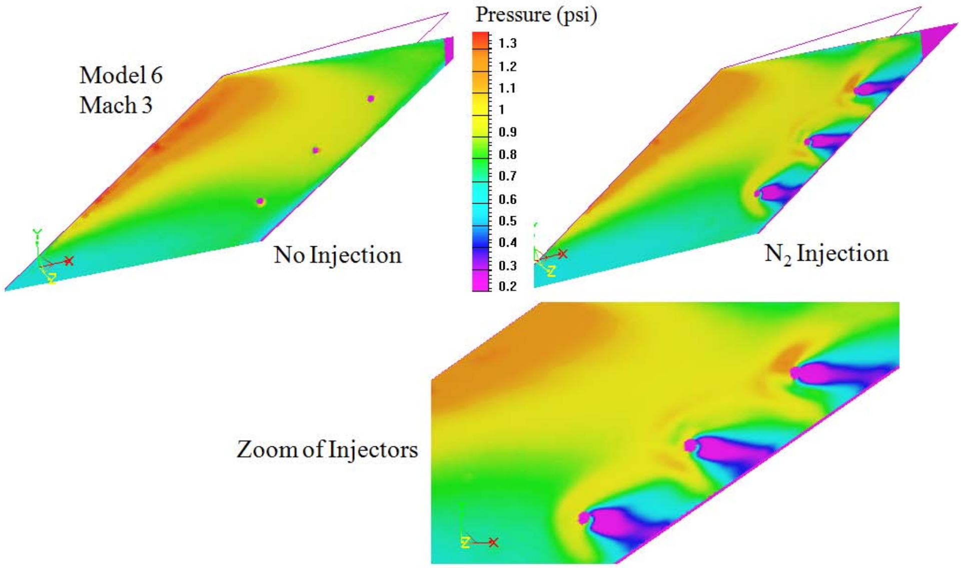
Pressure (psi)
1.3
1.2
1.1
1
0.9
0.8
0.7
0.6
0.5
0.4
0.3
0.2
Model 6
Mach 3
No Injection
N2 Injection
Zoom of Injectors